C. R. Mecanique 330 (2002) 91–99

# On the nature of the boundary layers instabilities in a flow between a rotating and a stationary disc

**Ewa Tuliska-Sznitko [a], Eric Serre [b], Patrick Bontoux [b]**

[a] **Institute of Thermal Engineering, Technical University of Poznan, 60-965 Poznan, Poland**

[b] **LMSNM CNRS-FRE 2405, IMT Château-Gombert, La Jetée, Université de la Méditerranée, 38, rue F. Joliot-Curie, 13451 Marseille cedex 20, France**

**Received 5 March 2001; accepted after revision 10 December 2001**

**Note presented by René Moreau.**

**Abstract** Both theoretical linear stability analysis and direct numerical simulation are performed to study the transition flow between a stationary and a rotating disc. This paper concerns three-dimensional spiral and annular patterns computed with a high-order (spectral) numerical method and related to Bödewadt layer instabilities. The characteristic parameters of these boundary layer patterns are compared to the theoretical results and interpreted in terms of type I and type II generic instabilities. Moreover, the absolute instability regions are also theoretically identified and the critical Reynolds numbers of the convective/absolute transition in both layers are given. ***To cite this article: E. Tuliska-Sznitko et al., C. R. Mecanique 330 (2002) 91–99.*** © 2002 Académie des sciences/Éditions scientifiques et médicales Elsevier SAS

**fluid mechanics / instability and transition in rotating flows / convective and absolute instability / direct numerical simulation / linear stability analysis**

## Sur la nature des instabilités de couche limite dans un écoulement entre un disque fixe et un disque tournant

**Résumé** La transition d'un écoulement inter-disques de type rotor–stator est étudiée au moyen de la simulation numérique directe et de l'analyse linéaire de stabilité, en utilisant des approximations spectrales. Ce papier est consacré à l'analyse des structures annulaires et spirales obtenues par une méthode numérique tridimensionnelle dans la couche limite de Bödewadt. Les paramètres caractéristiques de ces structures sont comparés aux résultats théoriques et interprétés en termes d'instabilités de type I et II. De plus, les régions absolument instables sont identifiées théoriquement et les nombres de Reynolds critiques à la transition convectif/absolu sont déterminés dans les deux couches de Bödewadt et d'Ekman. ***Pour citer cet article : E. Tuliska-Sznitko et al., C. R. Mecanique 330 (2002) 91–99.*** © 2002 Académie des sciences/Éditions scientifiques et médicales Elsevier SAS

**mécanique des fluides / instabilité et transition dans un écoulement en rotation / instabilité convective et absolue / simulation numérique directe / analyse linéaire de stabilité**

*E-mail addresses:* sznitko@sol.put.poznan.pl (E. Tuliska-Sznitko); serre1@l3m.univ-mrs.fr (E. Serre); bontoux@l3m.univ-mrs.fr (P. Bontoux).


S1631-0721(02)01432-8/FLA

## *Version française abrégée*

L'étude des couches limites en rotation constitue aujourd'hui encore un thème majeur de la mécanique des fluides (voir une revue dans Serre et al. [7]). En effet, en plus des nombreuses applications industrielles ou géophysiques, ces couches limites constituent un des prototypes les plus simples d'écoulement tridimensionnel et revêtent par là un caractère fondamental d'importance en particulier pour l'étude de la transition. Ainsi, plusieurs analyses de stabilité théorique leur ont été consacrées [4–6,17]. Alors que les travaux de Itoh [5] concernaient les configurations confinées inter-disques et la mise en évidence des structures d'instabilités en spirales et annulaires, les travaux de Lingwood [2,3,9] ont apporté des résultats expérimentaux et théoriques nouveaux relativement à la nature convectif/absolue de la transition de l'écoulement sur disque seul.

La présente étude comporte une approche combinée, non-linéaire par la simulation numérique directe (DNS) et linéarisée par une analyse de stabilité (LSA) pour l'écoulement de type rotor–stator. Cette configuration permet en particulier de mettre en évidence le caractère convectif/absolu de la transition en écoulement confiné.

Le modèle physique est défini par la hauteur inter-disques, $2h$, et par le rayon du disque, $R$. L'adimensionalisation du problème de Navier–Stokes est réalisée par rapport au taux de rotation et les paramètres géométrique et physique, sont le rapport de forme, $L = R/2h$, et le nombre de Reynolds, $\mathrm{Re} = \Omega(2h)^2/\nu$. La méthode de simulation numérique directe est basée sur approximation de type spectrale collocation-Chebyshev, dans les directions non-homogènes $(r, z)$ et de type Galerkin–Fourier dans la direction périodique azimutale. Le couplage vitesse–pression est traité au moyen d'un algorithme de projection et l'avancement en temps est assuré par un schéma du seconde ordre de type Adams–Bashfort Euler retardé. La méthode a été précédemment validée dans [11] et utilisée dans des configurations semblables Serre et al. [7].

L'étude de ce problème par l'analyse linéaire de stabilité (LSA) a permis en particulier de préciser la nature convective/absolue de l'instabilité suivant les valeurs des paramètres. La technique est dérivée des travaux de Sznitko [6] développés en convection thermique avec rotation. Le critère de détermination de la nature convective ou absolue de l'instabilité est basé sur les propriétés de la relation de dispersion dans les plans complexes du nombre d'onde, $k$, et de la fréquence, $\omega$ [12]. L'instabilité absolue est identifiée par la présence de singularités dans la relation de dispersion (notées « pinch-point »). Les résultats obtenus se situent bien par rapport à la récente étude de Feria [17] dans le cas des structures annulaires et qui montre l'effet de la prise en compte de l'écoulement non parallèle dans la couche limite de Bödewadt du disque fixe.

L'écoulement de base pour une telle configuration est de type Batchelor et composé de deux couches limites, de type Ekman près du disque tournant et de type Bödewadt près du disque fixe, séparées par un écoulement non-visqueux en rotation quasi-solide.

Les résultats de simulation et d'analyse de stabilité montrent que la première bifurcation est associée à l'instabilité de la couche limite du disque fixe. Les deux approches concordent pour montrer l'existence d'un $\mathrm{Re}_\delta$ critique dans la couche de Bödewadt, $\mathrm{Re}_\delta = r^*/\sqrt{\nu/\Omega}$ de l'ordre de 21–27, en accord avec les résultats expérimentaux [15] et mettant en évidence une zone d'écoulement stable au voisinage de l'axe de rotation (Fig. 1b). Dans la gamme des nombres de Reynolds les plus élevés, $\mathrm{Re}_\delta > 63.5$ ($L = 2$) et $\mathrm{Re}_\delta > 86.5$ ($L = 5$), correspondant à des couches de Bödewadt de plus grands rayons, la simulation met en évidence des structures spirales bien déterminées par rapport aux résultats de notre analyse de stabilité concernant l'instabilité de type I (Tableaux 1 et 2). Dans la gamme des valeurs intermédiaires, $33 < \mathrm{Re}_\delta < 63.5$ ($L = 2$) et $26.6 < \mathrm{Re}_\delta < 86.5$ ($L = 5$), la simulation révèle dans le sens de l'écoulement (centripète) une modification de la structure en spirale vers une structure annulaire correspondant bien à une instabilité de type II – les deux structures coexistant sur le stator ($L = 5$) (Fig. 1a).

Notre analyse de stabilité linéaire montre que, pour la gamme des $\mathrm{Re}_\delta$ étudiés par DNS ($\mathrm{Re}_\delta < 173$), la couche d'Ekman du rotor est convectivement instable, seulement, la transition convectif/absolue

étant obtenue pour une valeur élevée du nombre de Reynolds local, $\mathrm{Re}_\delta = 578$. La re-stabilisation de l'écoulement de la couche de Bödewadt au voisinage de l'axe de rotation éliminant toute perturbation rémanente dans l'écoulement aspiré par le disque tournant – la couche d'Ekman reste stable sur l'ensemble des simulations considérées. Il est à noter que dans le cas d'une cavité rotor–stator annulaire, nous avons précédemment observé [7] que, lorsque le moyeu interne situé en $r$ au-delà de la zone stable proche de l'axe ($\mathrm{Re}_\delta > 27$), il permet de transfèrer vers le rotor les structures issues de la couche de Bödewadt ce qui engendre l'instabilité de nature convective de la couche d'Ekman.

## 1. Introduction

Numerous works have been recently devoted to the investigation of the instabilities associated to the single rotating-disc [1–3] and to the differentially rotating discs [4–7]. In the case of rotor–stator flows, and for sufficiently high aspect ratios, the base flow is of Batchelor type, composed of both Ekman and Bödewadt boundary layers close to the rotating and the stationary disc, respectively, and separated by an inviscid core. The transition process is related to both type I and type II generic linear instabilities. The type I instability is due to the presence of an unstable inflection point in the boundary layer velocity profile. The mechanism for type II instability is related to the combined effects of Coriolis and viscous forces (see details in [8]). The convective nature of spirals in the Ekman layer has been experimentally demonstrated over a single rotating disc by studying the response of the flow to a local perturbation [3]. In addition, the convective/absolute nature of the transition in the layer of a single rotating disc has been evidenced in both theoretical and experimental studies [2,3]. For the rotating flow over an infinite stationary disc, Lingwood [9] also found theoretically the occurence of this convective/absolute transition. The recent experimental results of the instability of the flow between a stationary and a rotating disc, have also revealed that the flow exhibits a convective/absolute transition in a rotor–stator cavity [10].

In the present paper, a linear stability analysis (noted LSA) is performed in order to enlighten the numerical results obtained in a cylindrical rotor–stator cavity with respect to type I and type II instabilities. The characteristic parameters of the annular and spiral patterns exhibited by direct numerical simulation (noted DNS) are shown in good agreement with the theoretical results. Moreover, the absolute instability regions are also theoretically identified, extending the approach of Lingwood [2,3,9] for a single disc to the enclosed rotor–stator flow.

## 2. Geometrical and mathematical models

The geometrical model is a rotor–stator cylinder of radius $R$. The discs are bounded by a stationary cylinder of height $2h$. The rotor (upper disc) rotates at uniform angular velocity $\Omega = \Omega e_z$, $e_z$ being the unit vector. The governing equations are the 3D Navier–Stokes equations written in velocity–pressure formulation, together with the continuity equation and appropriate boundary and initial conditions. It is convenient to write these using a cylindrical polar coordinate system $(r, z, \varphi)$, with respect to a stationary frame of reference. The scales for the dimensionless variables of space, time and velocity are $[h, \Omega^{-1}, \Omega R]$, respectively. The two control parameters are the Reynolds number $\mathrm{Re} = \Omega(2h)^2/\nu$ and the aspect ratio $L = R/2h$ (in the DNS). Using LSA, the base solution is similar and the radius is accounted via the local Reynolds number.

## 3. Direct numerical simulation

The numerical solution is based on a pseudospectral collocation Chebyshev–Fourier Galerkin approximation. The use of the Gauss–Lobatto collocation points in both radial and axial directions allows an accurate description of the very narrow wall layers. The time scheme corresponds to a combination of the

second-order backward differentiation formula for the viscous diffusion term and of the Adams–Bashforth scheme for the non-linear terms. The velocity–pressure coupling is performed with a improved projection algorithm and the lack of physical boundary condition at the axis for the axisymmetric Fourier mode is dealt with a dependent variable transformation, see [11].

## 4. Linear stability analysis (LSA)

The disturbance equations are obtained by expressing the velocity and the pressure fields, as the superposition of the basic state and of a perturbation field. We assume the flow to be locally parallel and the perturbation quantities have the following normal-mode form.

$$\left[u', v', w', p'\right]^{\mathrm{T}} = \left[\hat{u}, \hat{v}, \hat{w}, \hat{p}\right]^{\mathrm{T}} \exp\left(\alpha^* r^* + m\varphi - \omega^* t^*\right) + cc \tag{1}$$

where $\hat{u}$, $\hat{v}$, $\hat{w}$, $\hat{p}$ are the dimensional amplitudes of the three components of velocity (in $r^*$, $z^*$, $\varphi$) and pressure respectively, $\alpha^*$ and $\beta^* = m/r^*$ are the components of wave number $k^*$ in the radial and circumferential directions respectively, $\omega^*$ is the frequency and $t^*$ is time. Asterisks denote the dimensional values. We investigate the stability of a Batchelor flow and the coordinate system is located on the disc under consideration. The linear stability analysis equations plus the homogeneous boundary conditions ($\hat{u}(z^*) = \hat{v}(z^*) = \hat{w}(z^*) = 0$ at $z^* = 0$ and $z^* = 2h$) constitute an eigenvalue problem which is solved in a global manner [6]. As in the DNS, a spectral collocation method based on Chebyshev polynomials is used for discretisation of the LSA equations.

The flow is impulsively excited at a given location in space and time and the response of the boundary layer shows whether the flow is absolutely or convectively unstable. The flow is defined as absolutely unstable if its impulse response grows with time at every location in space [12]. The response of a linear system to the forcing input can be determine by the Green function $G(x, t)$:

$$G(x, t) = \frac{1}{(2\pi)^2} \int_F \int_L \frac{\mathrm{e}^{\mathrm{i}(kx - \omega t)}}{D(k, \omega; \mathrm{Re}_\delta)} \,\mathrm{d}\omega \,\mathrm{d}k \tag{2}$$

where: $\mathrm{Re}_\delta = r^*/(\nu/\Omega)^{1/2}$, is the local Reynolds number based on the characteristic length of a viscous rotating layer. Path $F$ in the complex plane of wave number $k$ is initially taken to be the real axis. The contour $L$ in the complex frequency plane $\omega$ is chosen so that the causality is satisfied: $G(x, t) = 0$ everywhere when $t < 0$. From the asymptotic solution of the Fourier–Laplace integral (2) a general mathematical criterion has been derived to determine the nature of instability [12–14]. According to this criterion the absolute instability can be identified by singularities in the dispersion relation called pinch-points. The pinch-points are located in a process of consecutive contour deformations in which $L$ is deformed toward the lower half of the $\omega$ plane [13]. We have the following criteria for absolute instability: the flow is absolutely unstable if so-called absolute amplification rate $\omega_{0i}$ is positive ($\omega_{0i} > 0$). Additionally, for $L$ contour located high enough in the $\omega$ plane the spatial branches $k^+(\omega)$ and $k^-(\omega)$ must lie in different halves of the $k$ plane.

## 5. Numerical results. Annular and spiral patterns in a Bödewadt layer

The two chosen aspect ratios are $L = 2$ and $L = 5$. The numerical strategy consists in increasing step by step the rotation rate from the base steady state. In order to provide high-accurate numerical solutions, the grid refinement is rather large in both non-homogeneous $(r, z)$ directions: $N \times M = 64 \times 64$, $123 \times 123$, respectively, for $\mathrm{Re} = 4000$ ($L = 2$) and $123 \times 33$ for $\mathrm{Re} = 1600$ ($L = 5$). The number of Fourier modes is kept constant at $K = 48$. The time-step is $\delta t = 10^{-3}$. A relevant measure of the accuracy is given by the value of divergence of velocity which controls the incompressibility constraint, see [11]. In all the cases, this

value is less than $10^{-11}$ within the domain and $10^{-5}$ at the boundaries (where this is actually an estimate outside the computation domain).

### 5.1. Axisymmetric mode of instability

The first bifurcation is related to the axisymmetric mode of the Bödewadt layer, the Ekman layer on the rotating disc remaining stable. Annular patterns occur on the stator disc for $\mathrm{Re} = 4000$ ($L = 2$) and $\mathrm{Re} = 1600$ ($L = 5$).

For $L = 2$, the bifurcation is of Hopf type and the angular frequency $\sigma = \omega^*/\Omega = 0.9$ is very close to the rotation frequency ($\sigma = 1$). This solution is characterised by 4 to 5 pairs of circular vortices with a radial wavelength $10 \leqslant \lambda_r^*/\delta \leqslant 21$ increasing with the radius, where $\delta = \sqrt{\nu/\Omega}$. These vortices travel inward (indicated by a negative speed velocity) along the Bödewadt layer with a phase velocity varying over the range $-0.08 \leqslant V_\phi^*/\Omega r^* \leqslant -0.02$ ($V_\phi^*$ being measured from the numerical solutions). The vortices disappear at $r^*$, corresponding to local Reynolds number $\mathrm{Re}_\delta = 21$ ($\mathrm{Re}_\delta = r^*/\delta$, $\delta = (\nu/\Omega)^{1/2}$).

For $L = 5$, the bifurcation is not of Hopf type in concordance with the computations in [4] and the time-dependent solution involves several fundamental frequencies, the primary being $\sigma = 4$. The inward travelling vortices – of radial wavelength $8 \leqslant \lambda_r^*/\delta \leqslant 17$ – vanish at $\mathrm{Re}_\delta = 27$.

### 5.2. Three-dimensional mode of instability

By disturbing the previously described axisymmetric solutions (see details in [7]), a bifurcation takes place corresponding to a three-dimensional mode of the Bödewadt layer instability. The rotating disc layer and the near-axis region remains unperturbed as in the axisymmetric solution, in agreement with the local Reynolds number criteria. The orientation of the wave front is with respect to the azimuthal direction of the geostrophic flow measured in terms of the angle $\varepsilon$ which is defined positive when the wave is inclined towards the axis. The wavelength of the spiral patterns is defined by $\lambda^*$, as $\lambda^* = (2\pi r^*/n)|\sin\varepsilon|$, where $n$ is the number of arms over $2\pi$ at the radius $r^*$.

For $\mathrm{Re} = 4000$ ($L = 2$), 4 to 5 pairs of rolls of radial wavelength close to $\lambda_r = \lambda_r^*/\delta = 25$, develop in 6 spiral arms. The angle $\varepsilon$ significantly decreases with the radius, $7^\circ \leqslant \varepsilon \leqslant 25.7^\circ$. The corresponding wavelengths vary over the range $16.1 \leqslant \lambda^*/\delta \leqslant 28.5$. The temporal behaviour exhibits now a quasi-periodic flow with two major frequencies equal to $\sigma = 0.9$ and $\sigma = 2.8$. The critical Reynolds number $\mathrm{Re}_{\delta c}$ is roughly 33 on the stationary disc, i.e., very close to the experimental value given by Savas [15], $\mathrm{Re}_{\delta c} = 35$. During the transient period (only) axisymmetric patterns are also observed in the intermediate radial region corresponding to $33 \leqslant \mathrm{Re}_\delta \leqslant 63.5$ – while the axisymmetric rolls immediately transform into spiral structures further from axis, $\mathrm{Re}_\delta > 63.5$. After transient, the axisymmetric structures vanish and spiral arms only are observed after stabilization.

For $\mathrm{Re} = 1600$ ($L = 5$), coexisting stable circular and spiral patterns are observed inside the Bödewadt layer – associated to dislocation phenomena (Fig. 1a). The solution is time-dependent, with a dominant angular frequency nearly equal to the rotation frequency; 8 pairs of rolls of radial wavelength $8.8 \leqslant \lambda_r^*/\delta \leqslant 17$ decreasing with radius, move downstream to $\mathrm{Re}_\delta = 26.64$ with phase velocity $-0.27 \leqslant V_\phi^*/\Omega r^* \leqslant -0.02$ (Fig. 1b). For $26.64 \leqslant \mathrm{Re}_\delta \leqslant 86.5$, 5 circular waves evolve. As in recent experiments [10,16], spiral structures evolve at larger distance from the axis, $86.5 \leqslant \mathrm{Re}_\delta \leqslant 173$, with local angle varying, $7^\circ \leqslant \varepsilon \leqslant 28^\circ$; the spiral arms exhibit dislocations.

## 6. Linear stability analysis results

### 6.1. Type I and type II boundary layer instabilities

In order to analyse the formers numerical results in terms of type I and type II instabilities we focused on the characteristics of the instabilities which are shown to be the most unstable [9]. In the *Bödewadt layer* (stator), the onset of the type II instability has been found at $\mathrm{Re}_{\delta c\mathrm{II}} = 35.5$ with the wave angle

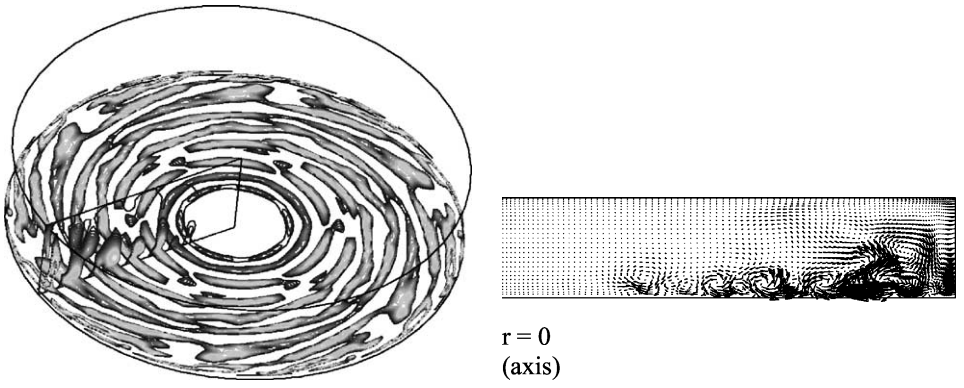


**Figure 1.** Co-existing annular and spiral patterns related to types II and I instabilities, respectively, of the Bödewadt layer. Cylindrical cavity $L = 5$, $\mathrm{Re} = 1600$. (a) Iso-lines of the fluctuations of the axial component. (b) Projection of the fluctuating velocity field in the plane $(r, z, \pi/4)$ emphasizing the most unstable zone of the Bödewadt layer $(26.64 \leqslant \mathrm{Re}_\delta \leqslant 173)$.

**Figure 1.** *Structures annulaire et spirale adjacentes relatives aux instabilités de types II et I, respectivement, de la couche de Bödewadt. Cavité cylindrique* $L = 5$, $\mathrm{Re} = 1600$. (a) *Iso-lignes des fluctuations de vitesse axiale.* (b) *Projection du champs de vitesse fluctuante dans le plan* $(r, z, \pi/4)$ *mettant en évidence la zone la plus instable de la couche de Bödewadt* $(26{,}64 \leqslant \mathrm{Re}_\delta \leqslant 173)$.

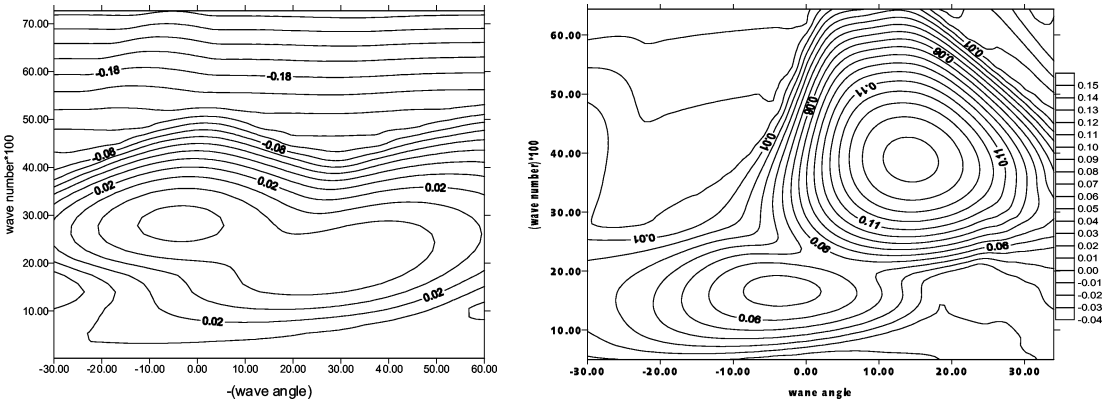


**Figure 2.** The iso-lines of $\omega_i = \text{const}$. (a) Stationary disc (Bödewadt layer), $\mathrm{Re}_\delta = 65$, (b) Rotating disc (Ekman layer), $\mathrm{Re}_\delta = 400$.

**Figure 2.** *Isolignes de* $\omega_i = \text{const}$. *à* $\mathrm{Re}_\delta = 400$. (a) *Couche limite du disque tournant.* (b) *Couche limite du disque fixe.*

$\varepsilon = -34.6°$, the wave-number's $k$ components $\alpha = \alpha^*\delta = 0.179$, $\beta = \beta^*\delta = -0.1237$ and the phase speed $V_\phi^*/\Omega r^* = \omega_r/k = -0.2526$ ($\sigma = \omega\,\mathrm{Re}_\delta$). The results have shown that type II instability can only exist in a narrow range of $\mathrm{Re}_\delta$, disappearing at $\mathrm{Re}_\delta = 68$. Type I instability occurs at $\mathrm{Re}_{\delta c1} = 47.5$ with $\varepsilon = \tan^{-1}(\alpha/\beta) = 0.8°$, $\alpha = 0.2959$, $\beta = 0.00413$, $\lambda_r = 21.23$ and $V_\phi^*/\Omega r^* = -0.06175$. The exemplary iso-lines of the temporal amplification rate $\omega_i$ in the plane of the wave-angle and number $(\varepsilon, k)$ obtained at the boundary layer of the stationary disc and also of the rotating disc are shown in Figs. 2a and 2b,

respectively. On the stationary disc, two separate regions of instability exist (Fig. 2a) at $\mathrm{Re}_\delta = 65$. The first pike obtained for higher wave-number with the maximum at $k \sim 0.28$ and $\varepsilon \sim 5°$ is identified as the type I instability. The second pike with maximum at $k \sim 0.2$ and $\varepsilon \sim -30°$ corresponds to the type II instability.

In the rotating disc flow, the onset of type II instability has been found at $\mathrm{Re}_{\delta c\mathrm{II}} = 90.23$ with $\varepsilon = -26.3°$, $\beta = -0.1098$, $\alpha = 0.222$ and $V_\phi^*/\Omega r^* = 0.39$. The type I instability occurs at $\mathrm{Re}_{\delta c\mathrm{I}} = 278.6$ with $\varepsilon = 10.9°$, $\alpha = 0.4173$, $\beta = 0.080322$ and $V_\phi^*/\Omega r^* = 0.0185$. Two separate regions of instability on the rotating disc at $\mathrm{Re}_\delta = 400$ are shown in Fig. 2b. The first pike, obtained for the lower wave-number with the maximum at $k = 0.177$ and $\varepsilon = -6.8°$, is identified as the type II instability. The second pike, with maximum at $k = 0.4$ and $\varepsilon = 12°$ corresponds to the type I instability.

Our linear stability results characterising the type I and type II instabilities are in very good accordance with Itoh's theoretical results [5] and also with the experimental results of Savas [15] who obtained $\mathrm{Re}_{\delta c\mathrm{II}} = 35.0$ in the case of the Bödewadt layer. Itoh [5] gives for the same geometrical configuration: $\mathrm{Re}_{\delta c\mathrm{II}} = 38.6$, $\mathrm{Re}_{\delta c\mathrm{I}} = 48.1$ for the Bödewadt layer and $\mathrm{Re}_{\delta c\mathrm{I}} = 281$, $\mathrm{Re}_{\delta c\mathrm{II}} = 85.3$ for the Ekman layer. The type I instability critical parameters are also in good agreement with the critical parameters obtained by Lingwood [9] for the stationary waves ($V_\phi^*/\Omega r^* = 0.0$) of the *Ekman layer*: $\alpha = 0.528$, $\beta = 0.137$, $\varepsilon = 14.5°$. However, there is a large difference between the present critical Reynolds numbers of the type I instability, $\mathrm{Re}_{\delta c\mathrm{I}} = 278.6$ and Itoh's one, $\mathrm{Re}_{\delta c\mathrm{I}} = 281$, and that obtained for the Ekman boundary layer by Lingwood $\mathrm{Re}_{\delta c\mathrm{I}} = 116.3$. This discrepancy is attributed to influence of the stationary disc in the configuration – contrasting to the open domain of Lingwood's Ekman flow.

### 6.2. Convective/absolute instability

The Briggs [12] criterion with a fixed wave number in the spanwise direction $\beta$ has been used in order to determine the region of absolute instability. The single disc case of Lingwood [9] has been considered in first. Indeed, Lingwood obtained for the Bödewadt layer $\mathrm{Re}_{\delta ca} = 21.6$, $\beta = -0.1174$, $\alpha_r = 0.34$, $\alpha_i = 0.0776$ and $\omega_r = -0.218$ whereas our critical parameters for this model are $\mathrm{Re}_{\delta ca} = 21.7$, $\beta = -0.1124$, $\alpha_r = 0.34$, $\alpha_i = 0.0806$ and $\omega_r = -0.213$. For the Ekman boundary layer we obtained exactly the same results as those published by Lingwood: $\mathrm{Re}_{\delta ca} = 198$, $\alpha_r = 0.379$, $\alpha_i = \pm 0.195$, $\beta = 0.184$, $\omega_r = \pm 0.039$. Comparison of the neutral curves of convectively and absolutely unstable areas obtained for the Bödewadt flow is presented in Fig. 3a.

Then, we have extended the Lingwood's case by considering the whole rotor–stator flow. As in the case of the single disc, almost the entire layer on the stationary disc is absolutely unstable (see the neutral curve

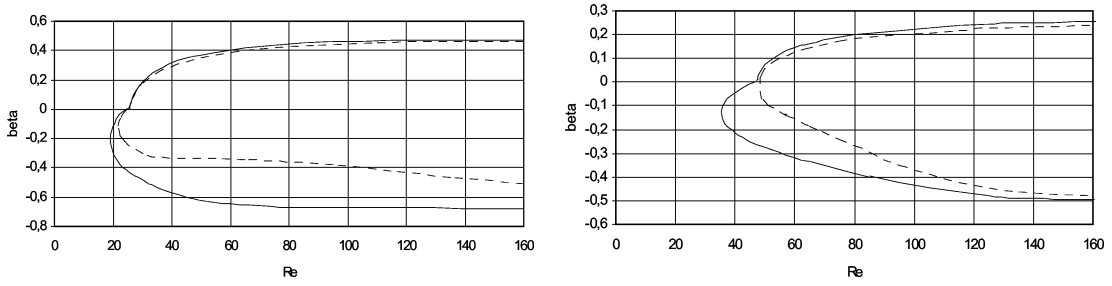


(a) (b)

**Figure 3.** Comparison of the neutral curves $\mathrm{Re}_\delta = f(\beta)$ of the absolutely (dashed line) and convectively (solid line) unstable flow obtained for: (a) the Bödewadt flow, (b) the stationary disc boundary layer.

**Figure 3.** *Comparaison des courbes neutres d'un écoulement absolument instable obtenu à partir de deux modèles, l'un prenant en compte l'écoulement entre deux disques et l'autre semi-infini sur un seul disque en rotation.* (a) *Couche limite du disque fixe.* (b) *Couche limite du disque en rotation.*

in Fig. 3b). The critical Reynolds number of the absolutely unstable flow has been found at $\mathrm{Re}_{\delta ca} = 48.5$ with $\beta = -0.0316$, $\alpha_r = 0.19$, $\alpha_i = 0.0569$ and $\omega_r = -0.0277$. On the rotating disc, the critical Reynolds number of the absolutely unstable flow is now determined at $\mathrm{Re}_{\delta ca} = 562$, which is more than 2.5 times larger than the value in Lingwood's case (with $\alpha_r = 0.26$, $\alpha_i = -0.143$, $\beta = 0.152$, $\omega_r = -0.0258$) showing the strong influence of the Bödewadt flow on the stability condition of the rotating disc layer. Moreover, we have found that the type II instability on the rotating disc remains totally convectively unstable in the presently configurations that we investigated using DNS.

## 7. Discussion and conclusion

The DNS calculations have shown that the first bifurcation of a confined rotor–stator flow is related to a Bödewadt layer instability and that the Ekman layer remains stable at least up to $\mathrm{Re}_\delta = 173$, considered in our study.

Travelling stable circular waves have been observed for $\mathrm{Re}_\delta > 21$ ($L = 2$, $\mathrm{Re} = 4000$) and for $\mathrm{Re}_\delta > 27$ ($L = 5$, $Re = 1600$). During the transient to a three-dimensional state ($L = 2$, $\mathrm{Re} = 4000$) circular patterns have also been temporarily obtained in the region corresponding to $33 < \mathrm{Re}_\delta < 63.5$. This range of $\mathrm{Re}_\delta$ agrees well with the range where type II is predicted to exist according to our LSA (i.e., $35.5 < \mathrm{Re}_\delta < 68.0$). The annular waves immediately mute into three-dimensional spiral vortices for higher $\mathrm{Re}_\delta$ where type I instability is dominant according to the linear stability analysis. The same good agreement between DNS and LSA results have been found for larger aspect ratio $L = 5$. In this case, circular and spiral patterns are

**Table 1.** Characteristic parameters of the type II instability of the Bödewadt layer. Present DNS and LSA results and literature results.

**Tableau 1.** *Paramètres caractéristiques de l'instabilité de type II de la couche de Bödewadt. Résultats de DNS et de LSA et résultats de la littérature.*

| Authors | $\mathrm{Re}_\delta$ | $\varepsilon$ | $\lambda_r$ | $V_\phi^*/\Omega r^*$ | $\mathrm{Re}_{\delta c\mathrm{II}}$ | $\sigma$ |
|---|---|---|---|---|---|---|
| Feria [17], PST | 19.8 | 0.0° | 13 | −0.22 | 19.8 | 2.1 |
| Itoh [5], LSA | [38.6; 55] | [−29.8°; −25.6°] | [34; 34.8] | [−0.23; −0.21] | 38.6 | [1.9; 2.3] |
| Savas [15], Exp. | 35 | 0.0° | 19 | −0.1 | 35 | 1.15 |
| Present DNS, $L = 2$ | [21; 126.5] | 0.0° | [10; 21] | [−0.08; −0.02] | 21 | 0.9 |
| Present DNS, $L = 5$ | [27; 173] | 0.0° | [8; 17] | [−0.13; −0.21] | 27 | 4 |
| Present LSA | [35.5; 60] | [−34.6°; −31.3°] | [35.1; 35.7] | [−0.25; −0.23] | 35.5 | [1.94; 2.8] |

**Table 2.** Characteristic parameters of the type I instability of the Bödewadt layer. Present DNS and LSA results and literature results.

**Tableau 2.** *Paramètres caractéristiques de l'instabilité de type I de la couche de Bödewadt. Résultats de DNS et de LSA et résultats de la littérature.*

| Authors | $\mathrm{Re}_\delta$ | $\varepsilon$ | $\lambda_r$ | $V_\phi^*/\Omega r^*$ | $\mathrm{Re}_{\delta c\mathrm{I}}$ | $\lvert\sigma\rvert$ |
|---|---|---|---|---|---|---|
| Itoh [5], LSA | [48.1; 200] | [−1.6°; 14°] | [23.7; 24.16] | [−0.077; −0.02] | 48.1 | 0.98 |
| Lingwood [9] | 27.4 | 13.3° | 13 | 0 | 27.4 | 0.00 |
| Present DNS, $L = 2$ | [63.2; 126.5] | [7°; 25.7°] | [28.5; 16.1] | [−0.062; −0.68] | 63.5 | 0.9; 2.8 |
| Present DNS, $L = 5$ | [86.5; 173] | [7°; 28°] | [8.8; 17] | [−0.02; −0.27] | 86.5 | 1 |
| Present LSA | [47.5; 200] | [0.8°; 10°] | [21.2; 24.35] | [−0.062; −0.018] | 47.5 | 0.9 |

both stable and coexist; *circular waves of type II* evolve in range $26.6 < \mathrm{Re}_\delta < 86.5$ while *type I spiral vortices* expand at larger $\mathrm{Re}_\delta$. Moreover, very recent theoretical results [17] that are based on spatial non-parallel linear calculations and devoted to the Bödewadt flow, also confirm that the annular structures near the stationary disc can be related to the type II instability. Indeed, the relevant parameters at the critical point, $\mathrm{Re}_{\delta c\mathrm{II}} = 19.8$, $\sigma = 2.1$ (i.e., $\omega = 0.106$), $\alpha = 0.482$, $\beta = 0.0$, $\varepsilon = 0.0°$, $V_\phi^*/\Omega r^* = -0.22$, that are determined by Feria [17], are very close to our characteristics numerically obtained. All the results are summarized in Tables 1 and 2.

Moreover, the absolute instability regions have also been theoretically identified in both layers. Our linear results have showed that the critical Reynolds numbers of the absolutely unstable flow are $\mathrm{Re}_{\delta ca} = 48.5$ and $\mathrm{Re}_{\delta ca} = 562$, for the Bödewadt and the Ekman layers, respectively. These results show that the Ekman layer is only convectively unstable for the parameter range considered in our DNS study. Consequently, as no perturbation is transferred from the Bödewadt layer – due to the presence of a stable flow region close to the axis, the Ekman layer remains stable. These results well complete the results of Lingwood [9] limited to the single disc case and extend the investigation to the case of the confined inter-disc flow. The convectively unstable character of the type II Ekman layer instability is also emphasized in our LSA results – which will the topic of a forth-coming paper.

**Acknowledgements.** CNRS support via Conseil Scientifique of IDRIS Computing Center is gratefully acknowledged. Computations were partly performed in Poznan Computer Center.

## References

[1] R. Kobayashi, Y. Kohama, Ch. Takamadate, Spiral vortices in boundary layer transition region on a rotating disk, Acta Mech. 35 (1980) 71–82.
[2] R. Lingwood, Absolute instability of the boundary layer on a rotating disk, J. Fluid. Mech. 299 (1995) 17–33.
[3] R. Lingwood, Experimental study of absolute instability of the rotating-disk boundary layer flow, J. Fluid. Mech. 314 (1996) 373–405.
[4] O. Daube, P. Le Quéré, R. Cousin, R. Jacques, Influence of curvature on transition to unsteadiness and chaos of rotor–stator disk flows, J. Fluid Mech. (2001) (soumis).
[5] M. Itoh, On the instability of the flow between coaxial rotating disks, in: Boundary Layer Stability and Transition to Turbulence, ASME FED, Vol. 114, 1991, pp. 83–89.
[6] E. Tuliszka-Sznitko, C.-Y. Soong, Instability of non-isothermal flow between coaxial rotating disks, in: Proceedings of European Congress on Computational Methods in Applied Sciences and Engineering, Barcelona, 2000.
[7] E. Serre, Crespo del Arco, P. Bontoux, Annular and spiral patters in flow between rotating and stationary disks, J. Fluid. Mech. 434 (2001) 65–100.
[8] D. Lilly, On the instability of Ekman boundary flow, J. Atmospheric Sci. 23 (1966) 481–490.
[9] R. Lingwood, Absolute instability of the Ekman layer and related rotating flows, J. Fluid. Mech. 331 (1997) 405–428.
[10] P. Gauthier, P. Gondret, M. Rabaud, Axisymmetric propagating vortices in the flow between a stationary and a rotating disk enclosed by a cylinder, J. Fluid Mech. 386 (1999) 105–127.
[11] E. Serre, J. Pulicani, A 3D pseudo spectral method for convection in a rotating cylinder, Computers and Fluids 30 (4) (2001) 491–519.
[12] R. Briggs, Electron-Stream Interaction with Plasmas, MIT Press, 1964.
[13] K. Kupfer, A. Bers, A. Ram, The cusp map in the complex – frequency plane for absolute instabilities, Phys. Fluids 30 (1987).
[14] P. Huerre, P. Monkewitz, Local and global instability in spatially developing flows, Annual Rev. Mech. 22 (1990) 473–537.
[15] O. Savas, Stability of Bödewadt flow, J. Fluid Mech. 183 (1987) 77–79.
[16] L. Schouveiler, P. Le Gal, M.P. Chauve, Y. Takeda, Spiral and circular waves in the flow between a rotating and a stationary disc, Experiments in Fluids 26 (1999) 179–187.
[17] F. Feria, Axisymmetric instabilities of Bödewadt flow, Phys. Fluids 12 (7) (2000) 1730–1739.